Skin Research and Technology 2013; 19: e297–e304
Printed in Singapore · All rights reserved
doi: 10.1111/j.1600-0846.2012.00643.x


Skin Research and Technology

# Diagnosis of BCC by multiphoton laser tomography

Stefania Seidenari[1], Federica Arginelli[1], Sara Bassoli[1], Jennifer Cautela[1], Anna Maria Cesinaro[2], Mario Guanti[1], Davide Guardoli[1], Cristina Magnoni[1], Marco Manfredini[1], Giovanni Ponti[1] and Karsten König[3,4]

[1]Department of Dermatology, University of Modena and Reggio Emilia, Modena, Italy,
[2]Department of Pathology, University of Modena and Reggio Emilia, Modena, Italy,
[3]Department of Biophotonics and Lasertechnology, Saarland University, Saarbrücken, Germany and [4]JenLab GmbH, Schillerstrasse 1, 0745, Jena, Germany

**Background/purpose:** Multiphoton Laser Tomography (MPT) is a non-linear optical technique that gives access to morphology and structure of both cells and extracellular matrix of the skin through the combination of autofluorescence imaging and second harmonic generation (SHG). The aim of this study was to identify MPT descriptors on *ex vivo* specimens of basal cell carcinoma (BCC) to assess the sensitivity and specificity of these criteria for the diagnosis of BCC and its differentiation from other skin tumours, inflammatory diseases and healthy skin.

**Methods:** In the preliminary study, MPT images referring to 24 BCCs and 24 healthy skin samples were simultaneously evaluated by three observers for the identification of features characteristic of BCC. In the main study, the presence/absence of the descriptors identified in the preliminary study was blindly evaluated on a test set, comprising 66 BCCs, 66 healthy skin samples and 66 skin lesions, including 23 nevi, 8 melanomas, 17 skin tumours and other skin lesions by 3 independent observers.

**Results:** In the preliminary study, three epidermal descriptors and six descriptors for BCC were identified. The latter included aligned elongated cells, double alignment of cells, cell nests with palisading and phantom islands. From the test set, 56 BCCs were correctly diagnosed, whereas in 10 cases the diagnosis was 'other lesions'. However, it was always possible to exclude the diagnosis of BCC in healthy skin and other lesion samples. Thus, overall sensitivity of the method was 84.85, whereas a specificity of 100% was observed with respect to both healthy skin and 'other lesions'.

**Conclusions:** This study describes new morphological descriptors of BCC enabling its characterization and its distinction from healthy skin and other skin lesions in *ex vivo* samples, and demonstrates for the first time that MPT represents a sensitive and specific technique for the diagnosis of BCC.

**Key words:** multiphoton laser tomography – basal cell carcinoma – skin tumours – tumour margins – extracellular matrix


Accepted for publication 26 April 2012

BASAL CELL carcinoma (BCC) is the most frequent skin cancer in humans and represents a major health concern especially in Caucasians (1, 2). The tumour rarely gives rise to metastases; however, it frequently arises on the face leading to local tissue destruction. Surgery is the treatment of election especially for invasive cancer, and has to be carried out possibly when the BCC is in an initial stage, sparing the surrounding healthy tissue as much as possible, although guaranteeing the total removal of the tumour (3). The identification of tumour margins also represents a challenge because most BCCs have poorly defined boundaries. Thus, both early recognition of small lesions and identification of tumour borders during surgery are of great practical importance.

When facing a suspicious lesion, the usual course of action comprises visual inspection followed by a biopsy and subsequent histopathological examination. This leads to delayed definitive surgical treatment.

For secure elimination of the entire cancer tissue, the technique of Mohs micrographic surgery, based on surgical removal and histology of successive tissue slices, is frequently used (4). However, this procedure is time consuming and costly. To circumvent these drawbacks, technological development has proposed real-time imaging methods, such as dermoscopy and confocal laser microscopy.

Dermoscopy, enabling the visualization of subsurface anatomic structures of the epidermis and papillary dermis, has become a popular imaging method because it is reliable, cost-effective and non-invasive (5). Confocal laser microscopy represents a 'third-level' technological aid further improving the diagnosis of BCC (6). Despite the introduction of these techniques, there still remains a 'grey' zone constituted by a certain number of cutaneous lesions that are difficult to classify (7). Therefore, new technologies are needed with the aim of further improving the diagnostic accuracy.

The non-linear optical technique of multiphoton tomography (MPT) imaging, employing an ultrafast laser for effective excitation of fluorescent materials, has been used for biological specimen imaging both *in vivo* and *in vitro* (8–16). Due to the non-linear excitation process, only the focal volume can be effectively excited by use of a near-infrared light source, allowing higher axial contrast, increased imaging depth and lower overall sample photodamage to be achieved. Efficient MPT excitation usually requires ultrashort femtosecond laser pulses, which are also able to produce the non-linear effect of second harmonic generation (SHG), engendered by periodic structures in tissue matrix components such as collagen. The combination of autofluorescence imaging and SHG gives access to morphology and structure of both cells and extracellular matrix of the skin.

The aim of this study was to identify MPT descriptors on *ex vivo* specimens of BCC. We also assessed the sensitivity and specificity of these criteria for the diagnosis of BCC and its differentiation from other skin tumours or inflammatory diseases and from healthy skin.

## Materials and Methods

*Study design*

The study was divided into two parts: a preliminary and a main study. In the former, MPT intensity images referring to 24 BCCs and 24 healthy skin samples were simultaneously evaluated by 3 observers (SS, MG and DG) for the identification of features characteristic of BCC.

In the main study, the presence/absence of the descriptors identified in the preliminary study was blindly evaluated on a test set, comprising 66 BCC, 66 healthy skin samples and 66 skin lesions, including 23 nevi, 8 melanomas, 17 skin tumours and 18 other skin lesions by 3 independent observers (FA, JC and MM), who also classified the images into those pertaining to BCC, healthy skin or 'other'. One field of view per sample and 10 images per field of view were examined (in total 1980 images).

The local ethics committee granted approval of the study protocol before the start of the study.

*Instrumentation: multiphoton tomography*

In this study, we used the MPT DermaInspect imaging system® (Jenlab GmbH, Jena, Germany), which provides intra-tissue scanning with subcellular spatial resolution (0.5 μm in lateral direction and 1–2 μm in the axial direction) (9, 10, 17). The CE-marked and commercially available imaging tool is rated as a class 1 M device according to the European laser safety regulations and consists of three major modules: laser, scanning-detector unit and control module. The laser source utilizes a mode-locked, 80 MHz, Ti:S (titanium:sapphire) laser (Mai-Tai; Spectra Physics, Mountain View, CA, USA) with a tuning range of 710–920 nm, a 75-fs pulse width and a maximum laser power of 900 mW that is attenuated to a maximum of 50 mW at the sample. The scanning-detector unit consists of a photodiode for electronic triggering, beam expander, fast *x–y* galvoscanners, a 40x focusing objective (NA = 1.3 oil) as well as a photomultiplier tube (PMT) for intensity imaging. A colour-glass filter (SCHOTT BG39, SCHOTT Italglas s.r.l, Genova) is employed in front of the PMT to block the scattered laser radiation light.

*Patients and skin samples*

The study included 90 BCC samples (66 nodular, 24 superficial) surgically removed from 86 patients (48 male and 38 female; age range 35–102 years) 59 lesions were located on face/neck/scalp, 23 on the trunk and 8 on the limbs. Among the BCCs, 32 were partially pigmented. In all cases, the clinical diagnosis was confirmed by conventional histopathological examination.

Each sample was excised during dermatological surgery, then cut, saving some healthy skin,

to obtain a regular shape, allowing its positioning under the microscope. The tissue specimens excised contained the entire skin lesion and normal perilesional skin from the ends of the spindle-shaped resection. For observation, saline solution was used as the immersion medium under the objective lens in order to maintain the natural tissue osmolarity.

*Image acquisition*

*Ex vivo* samples were placed on a cork disc covered by a transparent film and a gauze. For the examination of the samples a drop of water was placed between the skin and the cover glass, which was then attached to a metal coupling ring using circular adhesive tape. The metal coupler was magnetically connected to the MPT system after applying a drop of oil (Immersol$^{TM}$ 518F, Carl Zeiss Ltd., Standort Göttingen - Vertrieb, Göttingen, Germany). Two-dimensional horizontal images were acquired through optical sectioning, parallel to the tissue surface (i.e. in the *x–y* plane). After finding the correct level, the focus on a specific layer was found by means of the software JLScan_1100. The imaging depth was first pinpointed to the upper layer (stratum corneum). Virtually three-dimensional images, called *z*-stacks, were obtained by sequentially changing the plane of focus (*z*-level), thus scanning at different tissue depths. For the acquisition of stacks, a stepwise descent from the surface to a depth of approximately 200 μm was performed with an interval of 15 μm (Fig. 1). The maximum imaging depth corresponds to the working distance of the focusing optics of the DermaInspect® system (200 μm). Each optical section, consisting of 512 × 512 pixels, was imaged with a scanning time of 25.5 s/frame and an excitation power between 20 and 45 mW.

For selective imaging of keratinocytes and tumour cells, an excitation wavelength of 760 nm was applied, whereas for the study of the extracellular matrix, the excitation wavelength was shifted to 800–820 nm.

When imaging in the dermis, signals from both collagen fibres (SHG signal) and elastin fibres (autofluorescence) can be generated. Separation of these signals was accomplished by an optical filter (Semrock, BLP01-405R-25, ~0.04% transmission at 415 nm) that can be inserted into the beam path and that excludes the SHG component of the signal when exciting at up to 820 nm. Imaging was accomplished within 30 min from biopsy.

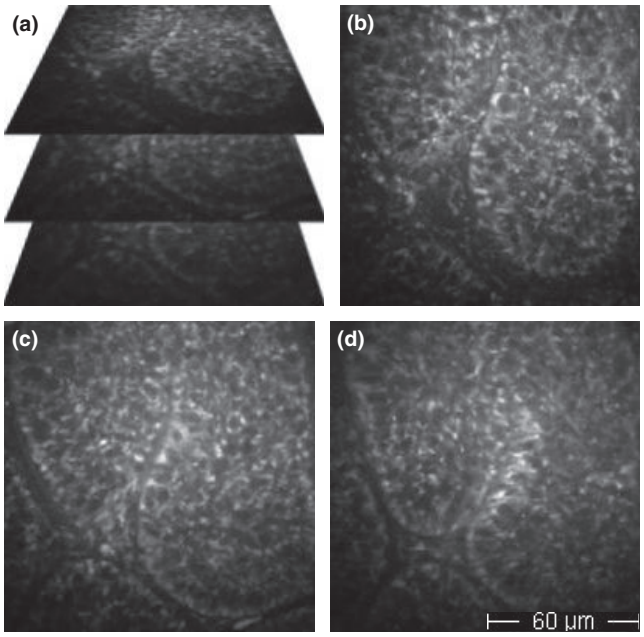


*Fig. 1. (a) Virtual three-dimensional image of a BCC. (b–d) Stacks from (b) to (d) are acquired employing an excitation wavelength of 760 nm; nests of basaloid cells are observable at different depths: (b) 100 μm, (c) 120 μm and (d) 140 μm. Cell nests appear with a peripheral aspect of palisading and they are surrounded by fibres and vessels.*

*Statistics*

The frequency of each descriptor in BCC, other skin lesion and healthy skin samples was computed. Sensitivity and specificity values of single or grouped descriptors and of the MPT diagnosis of BCC were evaluated compared with histopathologic diagnosis. Moreover, odds ratios (OD) were calculated for each descriptor. The agreement between ratings made by three observers on the diagnosis and specific patterns of BCC (inter-rater reliability) was estimated using Cohen kappa statistic with 95% confidence intervals. Statistical examinations were performed with SPSS 19.0 for Windows (SPSS Inc., Chicago, IL, USA). A $P$-value $< 0.05$ was considered statistically significant.

## Results

For each sample, 10 stacks were examined. In total, 900 images of BCC, an equivalent number of images of healthy skin samples and 660 images of different skin conditions were evaluated.

*Preliminary study*
After evaluation of 240 images corresponding to the stacks of 24 BCC samples, we identified 3 epidermal descriptors and 6 descriptors for BCC (Figs 2–4). When the lesion is not ulcerated and the epidermis is present, keratinocytes may exhibit jagged cellular contours and may have lost the normal cohesion. Intercellular spaces may be larger and uneven, and cells may be disposed in a random order (Fig. 2). When observing the tumour mass by an excitation wavelength of 760 nm, BCC cells show elongated shape and nuclei; they are monomorphous and aligned along the same direction; and tightly packed together (Fig. 3(a)). Divergent sheets of cells seem to crash one against the other giving rise to a double alignment (Fig. 3(b)). At the edge of the nodule, cells are lined up and closely packed and a palisading phenomenon is often visible (Fig. 3(c)). Basaloid nodules are observable as cell aggregates surrounded by fibres (Figs 1 and 3(d)). In some cases clear nests are not observable, but only sheets of cells intermingled with fibres (Fig. 3(e)). When shifting the excitation wavelength to 800–820 nm to explore the extracellular matrix, BCC cells disappear and only fibres surrounding black spaces are visible (phantom islands) (Figs 3(f) and 4).

*Main study*
The occurrence of each diagnostic feature was assessed by 3 independent observers on 66 BCC samples, 66 healthy skin samples and 66 lesions other than BCC. Absolute number and frequency of single descriptors, mean number of descriptors per lesion and frequency of the presence of at least one BCC descriptor and of BCC diagnosis are reported in Table 1. Mean number of descriptors per lesion was 2.64 in BCCs and 0.17 in other lesions.

*Sensitivity and specificity for BCC and healthy skin diagnosis*
A total of 56 BCCs were correctly diagnosed, whereas in 10 cases the diagnosis was 'other lesions'. However, it was always possible to exclude the diagnosis of BCC in healthy skin and other lesion samples. Thus, overall sensitivity was 84.85, whereas a specificity of 100% was observed with respect to both healthy skin and 'other lesions'. Moreover, healthy skin was always diagnosed as such.

*Sensitivity and specificity of BCC descriptors*
The presence of aligned elongated cells and double alignment showed a sensitivity of 73% and 61%, respectively, whereas lower sensitivity values were observed for cell islands, cells and fibres, phantom islands and palisading (Table 2). Specificity ranged 98.48 for 'sheets of cells intermingled with fibres' and 95.45 for 'cell islands surrounded by fibres'.

Table 3 shows sensitivity and specificity values of grouped MPT descriptors. By adding more criteria, sensitivity decreases because these criteria may not always be detected in all tumours. A sensitivity of 95.45 was achieved with one or more criteria, whereas a 100% specificity was obtained with four descriptors or more.

*Odds ratios*
Odds ratios of descriptors ranged from 100 for double alignment to 17.5 for cell islands surrounded by fibres (Table 2).

*Interobserver agreement*
The results of the kappa statistics analysis showed a good reliability of all criteria with kappa values ranging from 0.503 to 0.899 (Table 2).

## Discussion

BCC is a slow-growing epithelial skin tumour predominantly affecting middle-aged to elderly and fair-skinned individuals. Because its incidence is increasing worldwide, particularly in younger age groups, BCC emerges as a growing public health problem (1, 2). Early diagnosis enables a conservative treatment, whereas serious morbidity may result from an undiagnosed tumour.

Non-invasive procedures, such as dermoscopy, high-frequency ultrasound, optical coherence tomography and confocal microscopy, have been developed for improving the diagnosis of skin cancer. Because of its reliability and cost-effectiveness, dermoscopy has become the most widely used diagnostic technique in dermatologic practice to detect tumours at an early stage

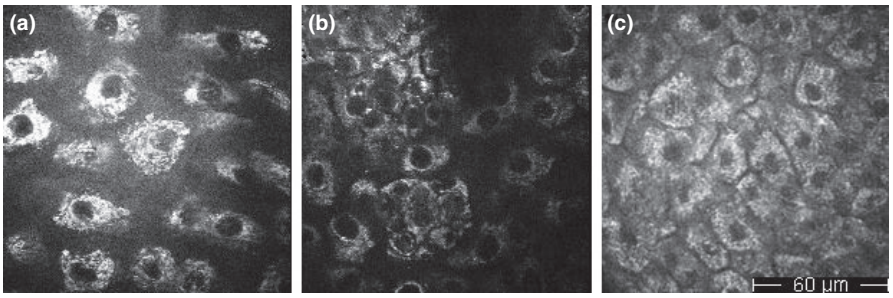


*Fig. 2. (a) Basal cell carcinoma acquired at 20 µm depth employing an excitation wavelength of 760 nm. In the upper layers basaloid cells have lost the normal cohesion; they are detached with large and irregular intercellular spaces. (b) Basal cell carcinoma acquired at 30 µm depth employing an excitation wavelength of 760 nm. Epidermal cells overlying the BCC show irregular contours and they are disposed in a random order. (c) Healthy skin at 20 µm depth employing an excitation wavelength of 760 nm. We can see the cohesion between keratinocytes disposed in a regular order.*

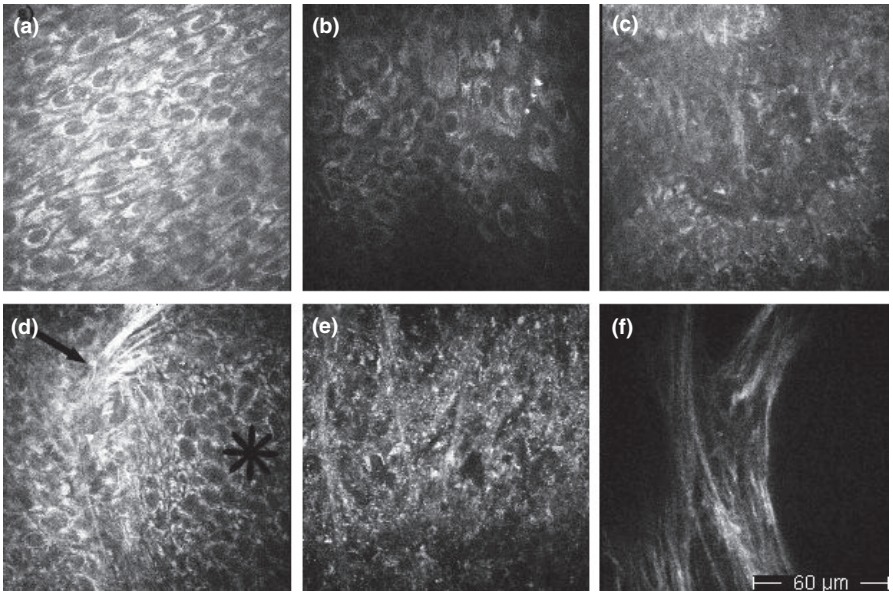


*Fig. 3. Descriptors of basal cell carcinoma. (a) 50 µm depth with an excitation wavelength of 760 nm. Basaloid cells are disposed in a regular order; they are aligned and elongated in the same direction, showing elongated shape and nuclei, and tightly packed together; (b) 50 µm depth with an excitation wavelength of 760 nm. Sheets of basaloid cells are elongated and aligned in two different directions; (c) 80 µm depth employing an excitation wavelength of 760 nm. At the periphery of basaloid nests, the cells are oriented perpendicularly to the surrounding extracellular matrix (palisading); (d) 90 µm depth with an excitation wavelength of 760 nm. A basaloid nodule (asterisk) is observable as a cell aggregate surrounded by fibres (arrow); (e) 30 µm depth employing an excitation wavelength of 760 nm: sheets of cells intermingled with fibres; (f) 75 µm depth with an excitation wavelength of 800 nm. Increasing the wavelength to 800 nm basaloid cells disappear and only the fibres of the extracellular matrix are visible (phantom island).*

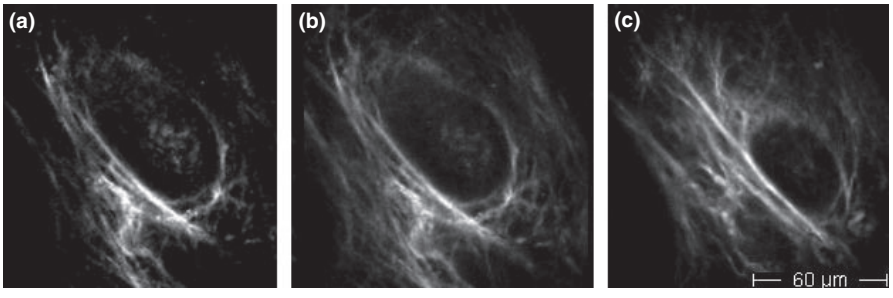


*Fig. 4. Basal cell carcinoma. (a) 100 µm depth, excitation wavelength 800 nm. Shifting the wavelength to 800 nm, basaloid cells become less visible; employing an excitation wavelength of 820 nm basaloid cells disappear and it is possible to observe empty spaces surrounded by collagen fibres (phantom island); (b) 100 µm depth; (c) 120 µm depth.*

*TABLE 1. MPT descriptors in samples of healthy skin (66), BCC (66) and other skin diseases (66)*

| | | BCC | | Miscellaneous | |
|---|---|---|---|---|---|
| | Healthy skin | *N°* | % | *N°* | % |
| Epidermal descriptors | | | | | |
| Detached cells with enlargement of intercellular spaces | 0 | 44 | 66.67 | 7 | 10.61 |
| Cells with irregular contours | 0 | 25 | 37.88 | 9 | 13.64 |
| Random arrangement | 0 | 24 | 36.36 | 6 | 9.09 |
| BCC descriptors | | | | | |
| Aligned elongated cells | 0 | 48 | 72.73 | 4 | 6.06 |
| Double alignment of monomorphous cells | 0 | 40 | 60.61 | 1 | 1.52 |
| Palisading | 0 | 23 | 34.85 | 1 | 1.52 |
| Cell islands surrounded by fibres | 0 | 30 | 45.45 | 2 | 3 |
| Sheets of cells intermingled with fibres | 0 | 12 | 18.18 | 1 | 1.52 |
| Phantom islands | 0 | 21 | 31.82 | 1 | 1.52 |
| Mean (+SD) number of BCC descriptors/lesion | | 2.64 ± 1.27 | | 0.17 ± 0.51 | |
| Presence of at least one BCC descriptor | | 63 | 95.45 | 11 | 16.67 |
| Diagnosis of BCC | 0 | 56 | 84.85 | 0 | 0 |

*TABLE 2. Sensitivity, specificity, Odds ratios (BCC vs. miscellaneous) and Cohen's k coefficients (including healthy skin evaluations) of the descriptors*

| | Sensitivity | Specificity | OR | 95% confidence interval | | Cohen's *k* coeffcients range |
|---|---|---|---|---|---|---|
| Aligned elongated cells | 72.73 | 96.21 | 57.57 | 17.85 | 185.63 | 0.503–0.899 |
| Double alignment | 60.61 | 97.73 | 100.00 | 13.06 | 765.81 | 0.642–0.745 |
| Palisading | 34.85 | 97.73 | 78.00 | 10.21 | 596.01 | 0.690–0.852 |
| Cells islands surrounded by fibres | 45.45 | 95.45 | 17.50 | 4.99 | 61.42 | 0.536–0.666 |
| Sheets of cells intermingled with fibres | 18.18 | 98.48 | 61.18 | 8.01 | 467.26 | 0.512–0.722 |
| Phantom islands | 31.82 | 97.73 | 69.06 | 9.04 | 527.49 | 0.657–0.725 |

*TABLE 3. Sensitivity and specificity of grouped MPT criteria*

| | Sensitivity | Specificity |
|---|---|---|
| $\geq 1$ | 95.45 | 88.63 |
| $\geq 2$ | 83.33 | 95.45 |
| $\geq 3$ | 53.03 | 99.24 |
| $\geq 4$ | 21.21 | 100 |
| $\geq 5$ | 10.60 | 100 |
| $\geq 6$ | 0 | 100 |

(5, 7). Arborizing telangiectasia, leaflike areas and large blue/grey ovoid nests represent reliable and robust parameters for BCC in dermoscopy and enable high sensitivity rates of dermoscopic diagnosis (5, 18, 19). Recent studies have emphasized the possible role of additional features, such as short fine telangiectasia and multiple small erosions, as further criteria for the dermatoscopic diagnosis of superficial BCC (20, 21).

BCC, however, may exhibit a large variety of characteristics that make clinical diagnosis difficult (22–25), and in particular some superficial BCCs may lack established dermoscopic criteria, which make dermoscopic diagnosis possible. Moreover, the resolution of dermoscopy does not always enable the identification of tumour margins.

These data indicate that an additional diagnostic method could be useful to investigate BCC prior to surgical excision both for a precise diagnosis and for tumour margin delimitation (26).

MPT should have high sensitivity, which is the ability of a test to correctly identify the presence of the disease, for it to be a valid screening test. It must also have high specificity, that is, the ability to correctly identify the absence of BCC. The aim of this study was to establish reliable BCC descriptors as assessed by MPT on *ex vivo* specimens, and to determine the sensitivity and specificity of these criteria for the diagnosis of BCC, with an aim to provide a useful adjunct *in vivo* modality for the diagnosis of BCC.

Employing MPT, the identification of healthy skin was achieved in 100% of the cases, rendering this technique a consistent tool for the definition of tumour margins. Moreover, specificity of the diagnostic criteria versus 'other lesions' was extremely high, indicating that the presence of at least one BCC descriptor makes the diagnosis of other lesions extremely unlikely. The identification of aligned elongated cells represented the most sensitive criterion showing at

the same time a very high sensitivity value, whereas to reach 99% specificity the presence of at least three descriptors was necessary.

Some MPT descriptors represent the equivalent of histopathological features, such as aligned elongated monomorphous cells, peripheral palisading of tumour cells and typical tumour islands. Other descriptors are identifiable only with this novel technique and cannot be recognized in fixed and stained specimens. In particular, the study of the extracellular matrix is only possible by performing a shift from the usual 760-nm excitation wavelength to 800 nm. This makes the orientation of collagen and elastin fibres visible. Whereas in healthy skin, straight fibres oriented along divergent directions appear at a depth of 80–100 μm underneath the ringed papillae corresponding to the dermal-epidermal junction, in BCC, fibres tightly embrace the basaloid nests, whose cells are no longer detectable, giving rise to 'phantom islands', that is, empty spaces surrounded by fibres. Although present only in 31% of our BCCs, this descriptor is extremely specific, being found in only one squamous cell carcinoma.

Multiphoton imaging is based on skin fluorescence, generated by several intrinsically fluorescent molecules, such as NADH, cholecalciferol, flavins, keratins, elastin and also collagen (8–14, 27). In a living cellular skin tissue, the main fluorescent contribution for excitation at 760 nm is most likely due to NAD(P)H, which is involved in mitochondrial activity, and melanin molecules, along with keratin, elastin and collagen fluorescence.

In our study the *ex vivo* modality was chosen because of the lack of technical facilities for the acquisition of lesions situated on small curved surfaces. Because most BCCs are located on the face, we decided to perform an *ex vivo* study to collect homogeneous and comparable data.

To date, only a few studies, considering a limited number of cases, have employed MPT to investigate *ex vivo* BCC. In their study performed on six BCC specimens, Paoli et al. (28) have already demonstrated that some histopathological features characteristic of BCC, such as elongated cells, nuclei polarization and peripheral palisading, can be observed by MPT imaging. Cicchi et al. (29) used a multidimensional nonlinear laser imaging approach to visualize *ex vivo* samples of BCC. In comparison with normal skin, BCC showed a blue-shifted fluorescence emission, a higher fluorescence response at 800-nm excitation wavelength and a slightly longer mean fluorescence lifetime.

Examining one BCC sample, De Giorgi et al. (30) noted that BCC cells exhibit a reduced fluorescent contrast between cytoplasm and nucleus, with respect to healthy skin cells.

In this study we describe new morphological descriptors of BCC enabling the characterization of BCC and its distinction from healthy skin and other skin lesions in *ex vivo* samples, and demonstrate for the first time that MPT represents a sensitive and specific technique for the diagnosis of BCC. A future application is represented by the use of MPT directly on the skin before biopsy and histological examination (so-called optical biopsy) to provide clinicians both with a diagnostic tool increasing the diagnostic accuracy and an alternative to Mohs surgery in the guidance of the surgical removal of BCCs.

## Acknowledgements

The authors thank Marcel Höfer of JenLab for his expert technical assistance.

*Funding sources*: The study was supported by the European Communities (grant agreement no. HEALTH-f7-2008-201577).

*Conflicts of interest*: Karsten König is the CEO of Jenlab.

## References

1. Roewert-Huber J, Lange-Asschenfeldt B, Stockfleth E, Kerl H. Epidemiology and etiology of basal cell carcinoma. Br J Dermatol 2007; 157: 47–51.
2. Leiter U, Garbe C. Epidemiology of melanoma and nonmelanoma skin cancer: the role of sunlight. Adv Exp Med Biol 2008; 624: 89–103.
3. Telfer NR, Colver GB, Morton CA. British Association of Dermatologists. Guidelines for management of basal cell carcinoma. Br J Dermatol 2008; 159: 35–48.
4. Mohs FE. Mohs micrographic surgery: a historical perspective. Dermatol Clin 1989; 7: 609–611.
5. Argenziano G, Soyer HP, Chimenti S et al. Dermoscopy of pigmented skin lesions: results of a consensus meeting via the Internet. J Am Acad Dermatol 2003; 48: 679–693.
6. González S, Tannus Z. Real-time in vivo confocal reflectance microscopy of basal cell carcinoma. J Am Acad Dermatol 2002; 47: 869–874.
7. Vestergaard ME, Macaskill P, Holt PE, Menzies SW. Dermoscopy compared with naked eye examination for the diagnosis of primary melanoma: a meta-analysis of stud-

ies performed in a clinical setting. Br J Dermatol 2008; 159: 669–676.
8. Denk W, Strickler JH, Webb WW. Two-photon laser scanning fluorescence microscopy. Science 1990; 248: 73–76.
9. Kollias N, Zonios G, Stamatas GN. Fluorescence spectroscopy of skin. Vib Spectrosc 2002; 28: 17–23.
10. König K, Riemann I. High-resolution multiphoton tomography of human skin with subcellular spatial resolution and picosecond time resolution. J Biomed Opt 2003; 8: 432–439.
11. Riemann I, Dimitrow E, Fischer P, Reif A, Kaatz M, Elsner P, König K. High resolution multiphoton tomography of human skin in vivo and in vitro. SPIE-Proc 2004; 5312: 21–28.
12. Schenke-Layland K, Riemann I, Damour O, Stock UA, König K. Two-photon microscopes and in vivo multiphoton tomographs. Powerful diagnostic tools for tissue engineering and drug delivery. Adv Drug Deliv Rev 2006; 58: 578–596.
13. Lin SJ, Jee SH, Dong CY. Multiphoton microscopy: a new paradigm in dermatological imaging. Eur J Dermatol 2007; 17: 361–366.
14. Becker W, Bergmann A, Biskup C. Multispectral fluorescence lifetime imaging by TCSPC. Microsc Res Tech 2007; 70: 403–409.
15. König K. Clinical multiphoton tomography. J Biophotonics 2008; 1: 13–23.
16. Dimitrow E, Riemann I, Ehlers A, Koehler MJ, Norgauer J, Elsner P, König K, Kaatz M. Spectral fluorescence lifetime detection and selective melanin imaging by multiphoton laser tomography for melanoma diagnosis. Exp Dermatology 2009; 18: 509–515.
17. Benati E, Bellini V, Borsari S et al. Quantitative evaluation of healthy epidermis by means of Multiphoton microscopy and FLIM. Skin Res Technol 2011; 17: 295–303.
18. Menzies SW, Westerhoff K, Rabinovitz H, Kopf AW, McCarthy WH, Katz B. Surface microscopy of pigmented basal cell carcinoma. Arch Dermatol 2001; 36: 1012–1016.
19. Altamura D, Menzies SW, Argenziano G, Zalaudek I, Soyer HP, Sera F, Avramidis M, DeAmbrosis K, Fargnoli MC, Peris K. Dermatoscopy of basal cell carcinoma: Morphologic variability of global and local features and accuracy of diagnosis. J Am Acad Derm 2010; 62: 67–75.
20. Giacomel J, Zalaudek I. Dermoscopy of superficial basal cell carcinoma. Dermatol Surg 2005; 31: 1710–1713.
21. Scalvenzi M, Lembo S, Francia MG, Balato A. Dermoscopic patterns of superficial basal cell carcinoma. Int J Dermatol 2008; 47: 1015–1018.
22. Ferrari A, De Angelis L, Peris K. Unusual clinical and dermoscopic features in two cases of pigmented basal cell carcinoma. J Am Acad Dermatol 2005; 53: 1087–1089.
23. Felder S, Rabinovitz H, Oliviero M, Kopf A. Dermoscopic differentiation of a superficial basal cell carcinoma and squamous cell carcinoma in situ. Dermatol Surg 2006; 32: 423–425.
24. Felder S, Rabinovitz H, Oliviero M, Kopf A. Dermoscopic pattern of pigmented basal cell carcinoma, blue-white variant. Dermatol Surg 2006; 32: 569–570.
25. Rossiello L, Zalaudek I, Cabo H, Ferrara G, Gabriel C, Argenziano G. Dermoscopic-pathologic correlation in an unusual case of pigmented basal cell carcinoma. Dermatol Surg 2006; 32: 1509–1512.
26. Caresana G, Giardini R. Dermoscopy-guided surgery in basal cell carcinoma. J Eur Acad Dermatol Venereol 2010; 24: 1395–1399.
27. Skala MC, Squirrell JM, Vrotsos KM, Eickhoff JC, Gendron-Fitzpatrick A, Eliceiri KW, Ramanujam N. Multiphoton microscopy of endogenous fluorescence differentiates normal, precancerous, and cancerous squamous epithelial tissues. Cancer Res 2005; 65: 1180–1186.
28. Paoli J, Smedh M, Wennberg AM, Ericson MB. Multiphoton laser scanning microscopy on non-melanoma skin cancer: morphologic features for future non-invasive diagnostics. J Invest Dermatol 2008; 128: 1248–1255.
29. Cicchi R, Massi D, Sestini S, Carli P, De Giorgi V, Lotti T, Pavone FS. Multidimensional non-linear laser imaging of Basal Cell Carcinoma. Opt Express 2007; 15: 10135–10148.
30. De Giorgi V, Massi D, Sestini S, Cicchi R, Pavone FS, Lotti T. Combined non-linear laser imaging (2-photon excitation fluorescence microscopy, fluorescence lifetime imaging microscopy, multispectral multiphoton microscopy) in cutaneous tumours: First experiences. J Eur Acad Dermatol Venereol 2009; 23: 314–316.

Address:
*Stefania Seidenari*
*Department of Dermatology*
*University of Modena and Reggio Emilia*
*Via del Pozzo 71*
*41124 Modena*
*Italy*
*Tel: +39594222924*
*Fax: +39594224271*
*e-mail: stefania.seidenari@unimore.it*